High bubble concentrations produced by ultrasounds in binary mixtures

Olivier Louisnard, Nathalie Lyczko, Fabienne Espitalier, M Urzedowski, Y Vargas-hernandez, C Sanchez-romero

High bubble concentrations produced by ultrasounds in binary mixtures

O. Louisnard [a,*], N. Lyczko [a], F. Espitalier [a], M. Urzedowski [a], Y. Vargas-Hernandez [b], C. Sanchez-Romero [b]

[a] *Centre Poudres et Procédés, Ecole des Mines d'Albi-Carmaux, 81013 Albi Cedex 09, France*
[b] *Laboratorio de Ultrasonidos, Universidad de Santiago de Chile, Casilia 307, Santiago-2, Chile*

Abstract

It was discovered that simultaneous insonification and air blowing of different aqueous binary solutions such as water/sodium-dodecyl-sulphate (SDS), water/methanol or water/potassium-sulphate yields a very concentrated bubble cloud invading the whole vessel in a few seconds. After the end of insonification, this cloudiness remained in the solution for about 1 min. The phenomenon was investigated by computer-treatment of solution pictures recorded every second after the end of insonification. Turbidity appeared to increase with ultrasound power, and also with SDS concentration. During the disappearance of the cloud, a turbidity front appeared rising and spreading upward. This front was studied in the characteristic plane and interpreted as a spatial segregation of different bubble sizes rising with different terminal velocities. The bubble sizes involved were estimated to about 10 μm. Adsorption of surface active species are invoked to explain the cloud formation and its abnormally slow disappearance, but the occurrence of the phenomenon for potassium-sulphate salt remains unexplained.

Keywords: Acoustic cavitation; Surfactants; Surface tension; Fragmentation; Dissolution

1. Introduction

Power ultrasound are known to produce cavitation bubbles in liquids. These bubbles emerge from gas nuclei stabilised in the bulk of the liquid or trapped in the vessel walls and solid impurities and multiply by a combination of several phenomena such as rectified diffusion, coalescence or fragmentation [1]. For 20 kHz ultrasound frequencies, the resulting bubble population can be seen by the unaided eye as they self-organise as clusters or filaments, generally near locations of maximum acoustic pressure [2,3].

In order to ensure a sufficient number of cavitation bubbles and to control their gas content, sonochemistry experiments generally involve a direct bubbling of the solution with some specific gas. Even in this case and although thousands of small bubbles appear in the liquid, the global void fraction stays small, and the whole solution rather transparent. Afterwards, when ultrasounds are switched off, the cavitation bubbles disappear on a time scale of the order of 1 s, most of them by dissolution under the effect of Laplace tension.

As we were performing sono-crystallization experiments on potassium-sulphate aqueous solutions, we discovered by chance a curious phenomenon: when combining insonification and air blowing, the solution took a milky aspect in a few seconds and its cloudiness remained for about 1 min after switching off ultrasounds. Repeating the same experiment with water/methanol and water/sodium-dodecyl-sulphate solutions, the same observation was done, and we concluded that the cloud was constituted of small bubbles.

To our knowledge, such a phenomenon has never been reported, and its singularity in the context of cavitation deserved further investigation. In this article, we propose an analysis of the cloud disappearance after the end of insonification and discuss the possible origins of its formation.

2. Experimental

The experimental set-up is presented in Fig. 1: a rectangular vessel of dimensions 5.5 cm × 5.5 cm × 8 cm

* Corresponding author.
E-mail address: louisnar@enstimac.fr (O. Louisnard).

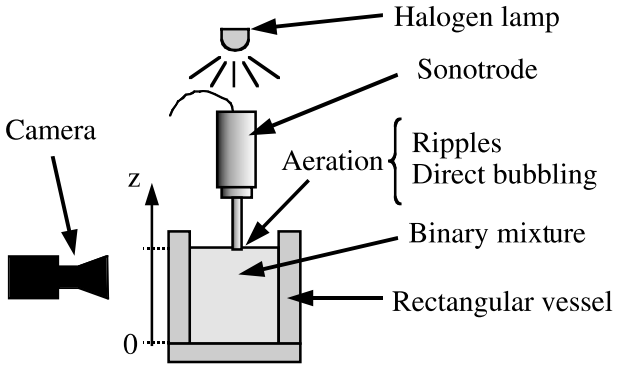

Fig. 1. Experimental set-up.

is partially filled up to 7 cm with a binary mixture. The following mixtures were tested:

- Water/sodium-dodecyl-sulphate (SDS) at two concentrations: 1/50th and 1/100th of the critical micellar concentration (8.3 mol/m^3) which we will denote SDS50 and SDS100 in the following.
- Water/potassium-sulphate with a concentration of 0.11 g/l, which we will denote K_2SO_4.

In all cases the initial temperature of the mixture was the temperature of the room (21°C ± 1°C). The solution was kept at rest for 30 min, between filling the vessel and starting insonification, and thrown out after each experiment. The vessel was insonified with a 13 mm titanium horn working at 20 kHz. Several acoustic amplitudes were used for every binary mixture. In order to compare different experiments, the voltage output of an uncalibrated hydrophone was recorded during separate experiments in the same vessel filled with pure water for different graduations of the generator amplitude control. Thus, in the following results, the acoustic pressure used in each experiment will be presented as a voltage.

Several methods were tested to feed the liquid with bubbles. The most natural one consisted in directly blowing air through a small piece of porous medium immersed in the vessel. A second less-intuitive method was performed by putting the tip of the transducer just at the air–liquid interface. Such an arrangement creates ripples at the liquid surface, so that air pockets were continuously trapped just under the transducer. This method yielded reproducible results and avoided the introduction of any foreign body in the liquid.

Then, in order to monitor the aspect of the solution during and after the insonification, the vessel was illuminated from above with a standard halogen lamp and the liquid was filmed from one side of the vessel with a classical 25 frames/s camera. For each experiment, the solution was insonified for 10 s, and a video sequence of 3 min was recorded.

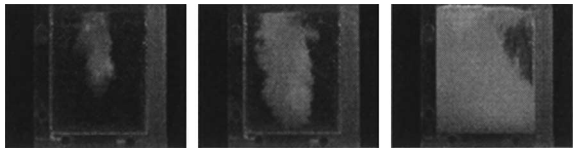

Fig. 2. State of the K_2SO_4 solution at different times after starting the insonification: from left to right: $t = 9/25$ s, $t = 13/25$ s, $t = 29/25$ s.

Fig. 2 shows the aspect of the liquid (water/potassium-sulphate) just after starting the insonification: turbidity appears immediately under the transducer and is then convected by acoustic currents to finally fill the whole volume of the vessel in less than 2 s.

Afterwards, once the ultrasound are switched off, the cloud gradually disappears (Fig. 3) on time scales of the order of 1 min. After a few seconds, a turbidity front emerges from the bottom of the vessel and slowly rises, leaving a transparency zone below. The same global behaviour was observed for all insonified binary mixtures, except for too low acoustic pressures where cavitation bubbles could be observed, but did not form any cloud.

The special arrangement of the transducer just at the surface of the liquid might yield a different acoustic energy transfer to the solution. This was checked in the K_2SO_4 solution by use of a calorimetric method for two different arrangements of the horn: from one hand with the tip located at the surface of the liquid, from the other

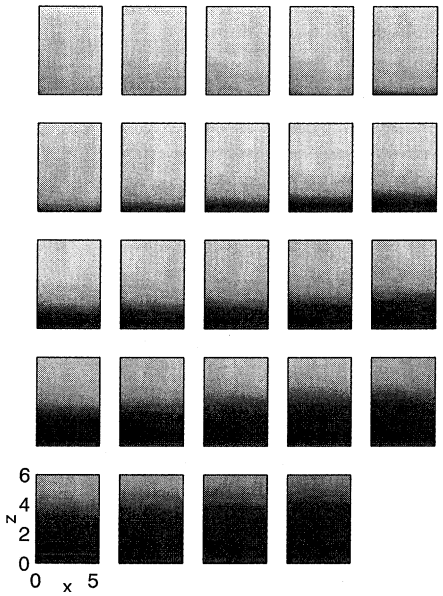

Fig. 3. State of the K_2SO_4 solution every 5 s after the end of insonification (from left to right and top to bottom) for the same experiment as Fig. 2. The top left image corresponds to the instant at which ultrasounds are switched off. The dimensions are indicated in cm on the left-bottom image.

Table 1
Dissipated power in the medium measured by calorimetry for two arrangements of the horn in the K_2SO_4 solution. The indicated voltage corresponds to the hydrophone output in pure water for the same graduation level of the generator

V (mV)	P (W), horn dipping	P (W), horn at the surface
131	44	32
145	62	48
157	100	78.3

hand with the tip dipped in the liquid. The results are shown in Table 1: it is seen that the former arrangement yields a lower dissipated power than the latter, which is the attended result since some fraction of the mechanical energy is used to create new interface in the medium. The difference between the two measures might be an indication of the total surface created but this has still to be demonstrated.

Larger insonification times (up to 20 min) were also used in order to check any effect on the phenomenon. No qualitative change was encountered in the phenomenon apart from a classical temperature increase.

3. Results

In order to get more insight in the process of bubble disappearance, images were extracted of the video sequences every second, and then treated by computer. First, colour images were converted to greyscale, and filtered by mean of a two-dimensional fast-Fourier-transform, in order to smooth non-significant high-frequency grey-level gradients. These grey-level values, ranging from 0 to 255, were then shifted by subtracting the average grey level of an image of the liquid at rest, so that a zero value corresponds to a transparent liquid. In this way, a spatio-temporal turbidity function $G(x,z,t)$ could be obtained for each experiment, where x represents the horizontal co-ordinate, z the height from the bottom of the vessel, and t the time since the end of insonification. This function does not represent directly the local void-fraction, but may be reasonably thought as a monotonic function (although non-linear) of the latter.

Several iso-value curves of the turbidity function $G(x,z,t)$ were calculated at each time and plotted in the (x,z) plane. An example is shown in Fig. 4 for the K_2SO_4 solution: it may be seen that except for the first seconds, the turbidity front is approximately monodimensional, indicating that all bubbles located at the same depth show approximately the same behaviour. Thus, the turbidity function may be reduced to a two-variables function $G(z,t)$, obtained by averaging over x the grey-level values at each z. The small departures from horizontality in the level curves of Fig. 4 may be

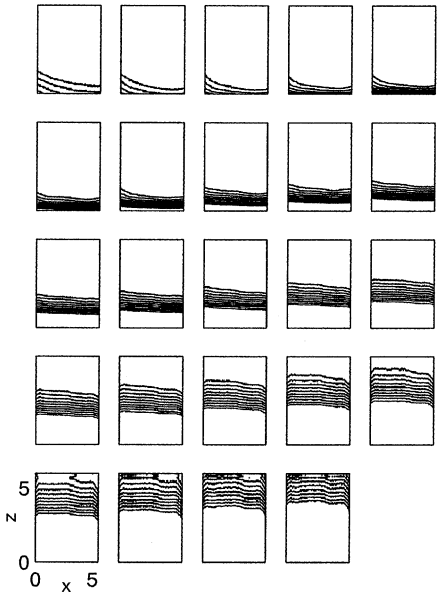

Fig. 4. Grey-level curves of the images of Fig. 3. Black regions correspond to a transparent solution, and white regions to a cloudy solution.

attributed to symmetry defects in the lighting method, in the location of the transducer and to wall effects.

The function $G(z,t)$ can be represented either as a function of depth at different times, or conversely as a function of time at different depths. The latter representation is shown in Fig. 5 for the SDS50 and SDS100 solutions: turbidity disappears in about 25 s for the SDS100 solution and in more than 100 s for the SDS50 one (note the log scales for the time axis). These results would indicate that the number of bubbles created during insonification is linked to the surfactant

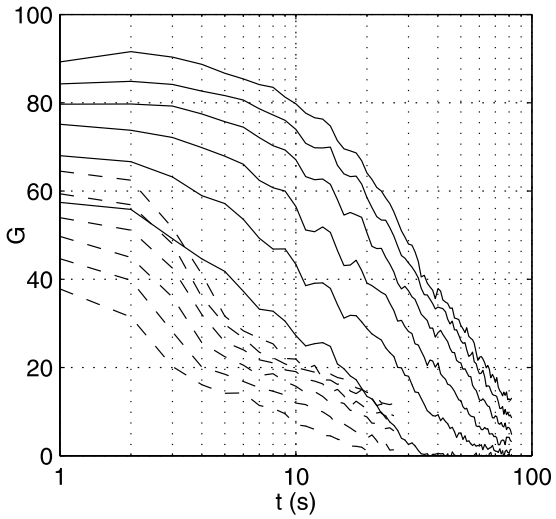

Fig. 5. Temporal evolution of turbidity of SDS50 solutions (—) and SDS100 solutions (- - -) at different depths in the vessel. Bottom to up: $z = 1, 2, 3, 4, 5, 6$ cm, where z is counted from the bottom of the vessel.

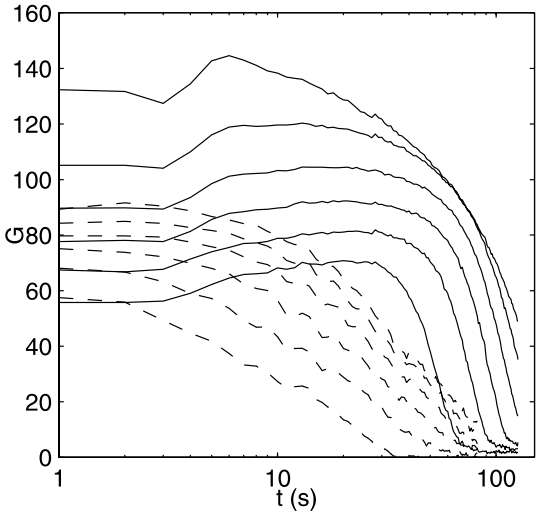

Fig. 6. Temporal evolution of turbidity of the K_2SO_4 solution (—) at the same levels as Fig. 5. Curves for SDS50 solutions are recalled (- - -) for comparison.

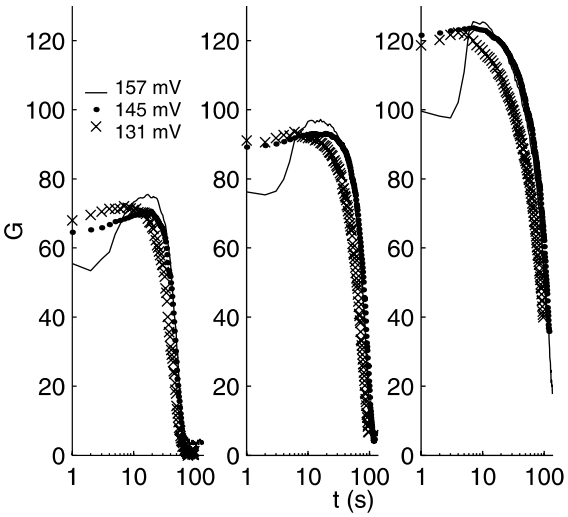

Fig. 8. Same as Fig. 7 for the K_2SO_4 solution.

concentration, and that the process has to do with surface tension. This will be discussed below.

Fig. 6 shows the same curves for the K_2SO_4 solution at the same power level. The curves for the SDS50 solution are recalled for comparison. It can be seen that turbidity is higher than for SDS solutions and that it disappears much more slowly.

The acoustic power was found to have a significant effect on the turbidity obtained. Fig. 7 shows the temporal evolutions of turbidity at three depths for SDS50 solutions insonified at three different ultrasound amplitude levels (the highest power level experiment was reproduced twice to show reproducibility): turbidity increases with ultrasound power. The same curves are reproduced, Fig. 8 for the K_2SO_4 solution: here two distinct stages may be observed: near the end of the disappearance process, the behaviour is similar as SDS experiments, and turbidity is higher for higher acoustic amplitudes but the effect is less pronounced than for SDS solutions. Conversely, at earlier stages, turbidity starts at a lower value for higher acoustic power, and increases for 10–25 s depending on the depth considered, at a rate increasing with the acoustic amplitude. This would mean that the void fraction increases temporarily at all depths, which is unlikely to occur. We suggest that this feature is an artefact of the lighting method used, since it was observed that for K_2SO_4 experiments, a thin layer of foam appeared at the liquid surface. This layer, which thickness increases with the acoustic level, could possibly screen the light emitted from above the vessel, and its disappearance would result in an apparent increase of the turbidity. This suggestion could be verified with more careful experiments.

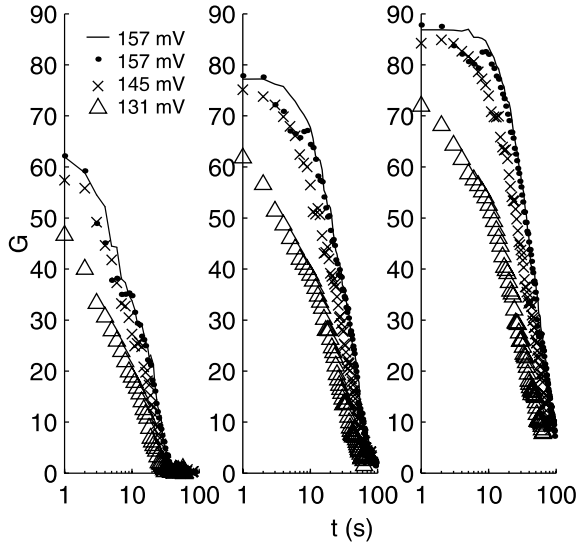

Fig. 7. Temporal evolution of turbidity of SDS50 solutions for different insonification amplitudes, at different depths: from left to right, $z = 1$, 3, 5 cm.

The qualitative behaviours described above do not tell much about the disappearance process. Particularly, to what extent the bubble cloud vanishes by rising or by natural dissolution remains undetermined. More can be learned from a careful examination of the turbidity front seen in Fig. 4. Such a spatio-temporal structure is reminiscent of non-linear waves problems, e.g. in gas dynamics, from which the characteristic curves representation can be borrowed [4]. For the experiment described on Fig. 2, several curves $G(z,t) = C^{te}$ are drawn in the (t,z) plane, (Fig. 9), for values of the constant ranging from 20 to 65 (compare with Y-axis of Fig. 6). It is seen that these curves originate approximately from the same point on the time axis, corresponding to the appearance of the front. Then they diverge from each other, bending slightly toward the increasing z.

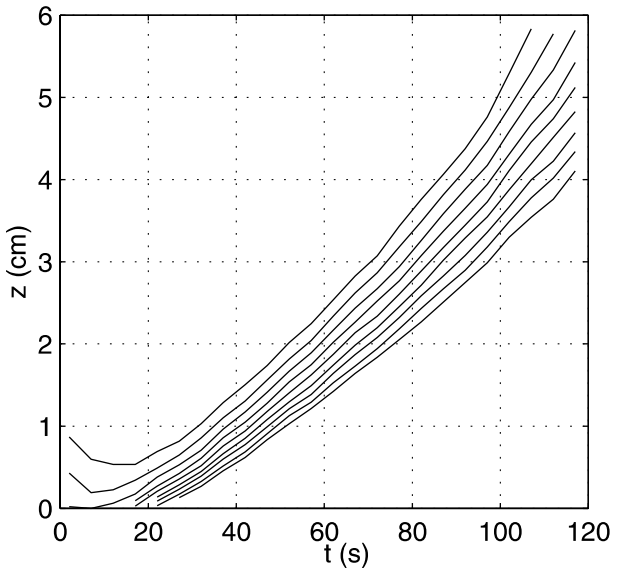

Fig. 9. Iso-value curves of the turbidity of the K_2SO_4 solution in the (t, z) plane. From bottom to top, the grey scale levels range from 20 to 65 by steps of 5.

These curves may be interpreted as follows: after the end of insonification, a distribution of several bubble sizes is present at the bottom of the vessel. These bubbles begin to rise by buoyancy, and after a short transient, they attain their terminal velocities, which depend on their respective sizes. For example, Stokes drag law predicts the following value:

$$v = \frac{9g}{2v} R_0^2 \tag{1}$$

This difference between the velocities of different-sized bubbles results in a progressive spatial segregation: the smallest bubbles form a slow lower layer, whereas bigger ones constitute upper layers travelling faster. If we assume that different sizes are approximately equally populated, this yield a void-fraction front (and also a grey-level front) initially very steep, and progressively spreading as the layers diverge from each other. This corresponds to the diverging characteristics observed in Fig. 9. The delay between the end of insonification and the appearance of the front may be attributed to residual convection induced by acoustic currents.

However, the characteristics should be linear since each bubble size rises with a constant velocity. The upward bending observed in Fig. 9 might be explained by the progressive slow dissolution of the bubbles as they travel upward. To make this point more clear, one may try to imagine what an observer should do to see always the same bubble size: if bubbles did not dissolve, such an observer would have to rise with constant velocity, but as the bubbles continuously decrease their size, he should accelerate to track upper bubbles currently dissolving to the observed size. This qualitative argument may be put on a more formal ground. Indeed, preliminary calculations [5] based on appropriate expressions of the dissolution rate and the terminal velocity, show that the (z, t) curves should scale as $z - z_0 \approx (t - t_0)^{5/3}$, which is approximately the case for the upper part of the curves shown in Fig. 9.

Of course, this reasoning is limited to the low turbidity values monitored in Fig. 9, which belong to a restricted interval. If we neglect dissolution, and relate the slopes of these curves to bubble velocities, one may obtain from Eq. (1) the different radii corresponding to the different iso-turbidity curves. We obtain values in the interval [10 μm, 15 μm], which order of magnitude is consistent with recent studies of cavitation bubble sizes in 20 kHz fields [6]. Besides, for such a narrow interval, the initial assumption of an approximate flat distribution function is reasonable.

It should be mentioned that larger bubbles may be present in the solution just after insonification and that they could contribute to the global turbidity of the solution. We just assert that they do not contribute to the front structure. Conversely, smaller bubbles may still be present in what we call the transparency region below the front, but their contribution to turbidity may be so small that our image analysis method could have missed them.

Hence, we get the important conclusion that the cloud persistence is mainly due to bubble sizes of the order of 10 μm, which disappear mostly by rising under buoyancy, and to a lesser extent by individual dissolution.

Although a front formation could also be observed in SDS experiments, this type of analysis was less successful, since turbidity is much lower and the front less pronounced. Further experiments with higher SDS concentrations should be done.

Finally, the comparison between the characteristic curves of K_2SO_4 for different insonification powers did not show any meaningful difference in the slopes of the curves.

4. Discussion

Following these observations, two basic questions remain unanswered:

- Why do so numerous bubbles appear in an insonified binary solution and not in pure water?
- Why do they not dissolve immediately after the end of insonification?

One may suggest that the whole process is a consequence of a surface effect. It is well-known that bubbles oscillating radially may undergo surface instabilities and

possibly fragment [7–9], either in an implosion phase, or by parametric amplification. For lower surface tension, bubbles are less stable and more likely to break-up. Thus, if surface tension is reduced, large bubbles blown in the solution may break-up into a cloud of small bubbles before they escape by buoyancy. Afterwards, these smaller bubbles may be easily convected by acoustic currents to fill the whole vessel.

On the other hand, the natural dissolution of a bubble in a liquid at rest is driven by a gas concentration gradient that results from the Laplace tension $2\sigma/R_0$, proportional to surface tension. If the latter is reduced, the dissolution time of bubbles is increased, and this may explain, at least qualitatively, why the bubble constituting the cloud stay so long in the solution after the end of insonification.

One may now ask why surface tension is reduced in the binary mixtures studied. The answer is natural in the case of SDS solutions since this molecule is a classical surface agent, so that it adsorbs to air–liquid interfaces, especially at the bubbles walls. Methanol, and more generally short-chain alcohols, is also known to have weak surface-active properties and can exhibit the same behaviour. For a given bulk concentration of such molecules in a liquid at rest, the surface concentration and the resulting surface tension may be calculated from sorption isotherms [10]. Moreover, as shown recently [11], adsorption of surface-active molecule at the wall of a bubble may be greatly enhanced by its radial oscillatory motion, even for weak bulk concentrations. Hence we suggest that this rectified adsorption process may occur during the insonification phase, so that a more concentrated layer of surface-active molecules would surround the bubbles constituting the cloud at the end of insonification. This layer should then desorb partially as soon as ultrasounds are switched off, to reach again the sorption equilibrium in a liquid at rest. The desorption kinetic may be slower than the diffusional one and may protect the bubble against dissolution for a sufficiently long time. This is supported by the above observations on SDS mixtures, which showed a more rapid dissolution for less concentrated solutions.

However, this interpretation suffers from a serious drawback: potassium-sulphate is known to have the opposite effect than surface agents, and should leave the air–liquid interfaces, increasing surface tension. Informal experiments have shown that other salts, like sodium-chloride, dissolved in small amounts in water also produce a cloudy aspect in the solution. One may argue that air solubility in salt solutions decreases with salt concentration and thus, a freshly prepared solution would be slightly supersaturated in air. Hence, the concentration gradient driving dissolution in still water would be reduced, possibly resulting in more stable bubbles. This argument does not explain however why the bubble cloud is so easily created. Other phenomena, like electrostatic interactions, may also be examined. The question remains open.

5. Conclusion

We have shown that the combined insonification and air blowing in binary aqueous mixtures produces a very concentrated bubble cloud in the solution, remanent for about 1 min after the end of insonification.

The formation of the cloud along with its unexpected stability after the end of insonification was interpreted by an ultrasound-enhanced adsorption process of surface agents at the bubble walls. Whereas this suggestion is plausible for water/sodium-dodecyl-sulphate and water/methanol binary mixtures, it is unable to explain why the phenomenon is still observed with water/potassium-sulphate mixtures. Further experiments have to be done with other salt mixtures and salt concentrations in order to determinate which physico-chemical properties are required to achieve the phenomenon.

The disappearance of the cloud seems to be due essentially to the rising of the bubbles under buoyancy, resulting in the formation of a turbidity front rising and spreading toward the surface of the liquid. The size of the bubbles in this turbidity front was estimated to about 10 μm, which is the order of magnitude of cavitation bubble sizes in 20 kHz acoustic fields.

As a concluding remark, we would like to suggest a possible application of the above-described phenomenon: ultrasound experiments are often said to be limited by an insufficient number of active bubbles. The number of active bubbles remains limited because these bubbles must emerge from the growth and fragmentation of nuclei initially present in the solution, but not so numerous. Bubbling the liquid is usually rather considered as a way to dissolve more gas, than to create more interface. The above results show that adding a small amount of some specie enables to create much more interface, which may then serve to create more transient bubbles. The cloud formation occurs in a few seconds, and could be repeatedly produced by a pulsed ultrasound source, while an immersed continuous one would transform some of these bubbles to transient ones.

Acknowledgements

We are grateful to the Association Française pour la Valorisation de la Recherche (ANVAR) for financial support, and to the Service Culturel et de Coopération Scientifique et Technique of the French Embassy for supporting exchanges between the School of Mines of

Albi and the Laboratory of Ultrasounds of the University of Santiago de Chile.

References

[1] T.G Leighton, Bubble population phenomena in acoustic cavitation, Ultrason. Sonochem. 2 (1995) S123–S136.
[2] W.L. Nyborg, D.E. Hughes, Bubble annihilation in cavitation streamers, J. Acoust. Soc. Am. 42 (1967) 891–894.
[3] U. Parlitz, C. Scheffczyk, I. Akhatov, W. Lauterborn, Structure formation in cavitation bubble fields, Chaos, Solitons Fractals 5 (1995) 1881–1891.
[4] G.B. Whitham, Linear and Nonlinear Waves, Wiley/Interscience, New York, 1974.
[5] O. Louisnard, in preparation.
[6] F. Burdin, N.A. Tsochatzidis, P. Guiraud, A.M. Wilhelm, H. Delmas, Characterisation of the acoustic cavitation cloud by two laser techniques, Ultrason. Sonochem. 6 (1999) 43–51.
[7] A.I. Eller, L.A. Crum, Instability of the motion of a pulsating bubble in a sound field, J. Acoust. Soc. Am. 47 (1970) 762–767.
[8] A. Prosperetti, Viscous effects on perturbed spherical flows, Q. Appl. Math. 34 (1977) 339–352.
[9] S. Hilgenfeldt, D. Lohse, M.P. Brenner, Phase diagrams for sonoluminescing bubbles, Phys. Fluids 8 (1996) 2808–2826.
[10] C.H. Chang, E.I. Franses, Adsorption dynamics of surfactants at the air/water interface: a critical review of mathematical models, data, and mechanisms, Colloids Surf. A 100 (1995) 1–45.
[11] M.M. Fyrillas, A.J. Szeri, Surfactant dynamics and rectified diffusion of microbubbles, J. Fluid Mech. 311 (1996) 361–378.